Interaction of *Escherichia coli* DNA Polymerase I with AzidoDNA and Fluorescent DNA Probes: Identification of Protein–DNA Contacts†

Carlos Enrique Catalano,‡ Dwayne J. Allen, and Stephen J. Benkovic*

Department of Chemistry, 152 Davey Laboratory, The Pennsylvania State University, University Park, Pennsylvania 16802

Received September 5, 1989; Revised Manuscript Received November 27, 1989

ABSTRACT: The synthesis of an azidoDNA duplex and its use to photolabel DNA polymerases have been previously described (Gibson & Benkovic, 1987). We now present detailed experiments utilizing this azidoDNA photoprobe as a substrate for *Escherichia coli* DNA polymerase I (Klenow fragment) and the photoaffinity labeling of the protein. The azidoDNA duplex is an efficient substrate for both the polymerase and 3′ → 5′ exonuclease activities of the enzyme. However, the hydrolytic degradation of the azido-bearing base is dramatically impaired. On the basis of the ability of these duplexes to photolabel the enzyme, we have determined that the protein contacts between five and seven bases of duplex DNA. Incubation of azidoDNA with the Klenow fragment in the presence of magnesium results in the in situ formation of a template-primer with the azido-bearing base bound at the polymerase catalytic site of the enzyme. Photolysis of this complex followed by proteolytic digestion and isolation of DNA-labeled peptides results in the identification of a single residue modified by the photoreactive DNA substrate. We identify Tyr766 as the modified amino acid and thus localize the catalytic site for polymerization in the protein. A mansyl-labeled DNA duplex has been prepared as a fluorescent probe of protein structure. This has been utilized to determine the location of the primer terminus when bound to the Klenow fragment. When the duplex contains five unpaired bases in the primer strand of the duplex, the primer terminus resides predominantly at the exonuclease catalytic site of the enzyme. Removal of the mismatched bases by the exonuclease activity of the enzyme yields a binary complex with the primer terminus now bound predominantly at the polymerase active site. Data are presented which suggest that the rate-limiting step in the exonuclease activity of the enzyme is translocation of the primer terminus from polymerase to exonuclease catalytic sites.

Replication and repair of DNA in *Escherichia coli* are mediated, at least in part, by DNA polymerase I (Pol I)[1] (Kornberg, 1980). This enzyme catalyzes the 5′ → 3′ addition of dNTP's onto a primer strand directed by a DNA template. The enzyme also effects DNA degradation with an associated 3′ → 5′ exonuclease activity. This exonuclease activity is thought to work in concert with the polymerase activity to ensure the high fidelity in DNA replication exhibited by the enzyme. Additionally, the enzyme possesses a distinct 5′ → 3′ exonuclease activity which is thought to play a role in the DNA repair functions of the enzyme (Setlow & Kornberg, 1972).

All of these catalytic activities reside on a single 103-kDa polypeptide chain (Jovin et al., 1969) that can be cleaved by limited proteolysis into two fragments (Brutlag et al., 1969; Klenow & Henningsen, 1970). The small fragment retains the 5′ → 3′ exonuclease (repair) activity while the polymerase and 3′ → 5′ exonuclease (editing) activities remain associated with the large 68-kDa fragment known as the Klenow fragment. A plasmid that overproduces the Klenow fragment has been constructed (Joyce & Grindley, 1983) and the X-ray crystal structure solved to 3.3 Å (Ollis et al., 1985). This structure reveals two distinct domains. The larger domain of the protein presents a large, deep cleft of the appropriate size and dimension to bind a DNA duplex. Electrostatic field calculations (Warwicker et al., 1985) show a net positive charge within this cleft and an overall negative charge over the remaining surface of the protein. Two metal ions are bound within the smaller of the two domains.

The 3′ → 5′ exonuclease activity of the enzyme is selectively inhibited by dNMP's (Que et al., 1978), suggesting that these nucleotides interact only with the exonuclease catalytic site. Cocrystal X-ray structures with dTMP (Ollis et al., 1985) show that this nucleotide binds exclusively within the small domain of the protein associated with the bound metal ions. These data argue that the 3′ → 5′ exonuclease catalytic site is located within the small domain of the protein. Strong support for this suggestion is provided by experiments in which the mononucleotide binding site has been removed by site-specific mutagenesis (Derbyshire et al., 1988). These mutant proteins exhibit perfectly normal polymerization kinetics but are devoid of exonuclease activity.

† This work was supported by NIH Grant GM13306 (S.J.B. and D.J.A.) and NIH Postdoctoral Fellowship GM11590 (C.E.C.).

* Address correspondence to this author.

‡ Present address: School of Pharmacy, University of Colorado, Box 297, Boulder, CO 80309.

[1] Abbreviations: Pol I, *Escherichia coli* DNA polymerase I; dNTP, deoxynucleoside 5′-triphosphate; 11az/20mer, the azidoDNA photoprobe used in these studies (see Chart I); 10az/20mer, the $n - 1$ exonuclease product of the 11az/20mer; 12az/20mer, 14az/20mer, 17az/20mer, and 20az/20mer, the $n + 1$, $n + 3$, $n + 6$, and $n + 9$ elongation products, respectively, of the 11az/20mer; 11*mer single-stranded DNA, a mansyl-bearing fluorescent DNA oligonucleotide (see Chart II, primer strand only); 22*mer single-stranded DNA, a mansyl-bearing fluorescent DNA probe used in these studies (see Chart II, primer strand only); 22*/31 correct, the mansyl-DNA probe containing a correctly matched primer terminus (see Chart II); 22*/31 mismatch, the mansyl-DNA probe containing an incorrectly matched primer terminus (see Chart II); mansyl, 6-(*N*-methylanilino)naphthalene-2-sulfonate; FPLC, fast protein liquid chromatography; HPLC, high-pressure liquid chromatography; kDa, kilodalton(s); EDTA, ethylenediaminetetraacetic acid; Tris-HCl, tris(hydroxymethyl)aminomethane hydrochloride; TEAA, triethylammonium acetate; TEAB, triethylammonium bicarbonate.

0006-2960/90/0429-3612$02.50/0

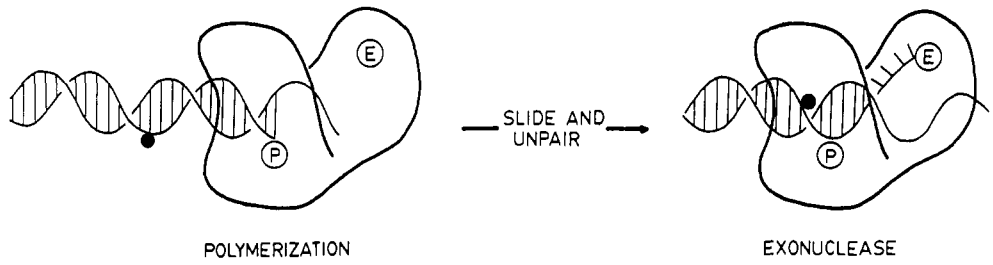

FIGURE 1: Model proposed for binding of the primer terminus to the exonuclease site of the enzyme [adapted from Freemont et al. (1988)]. Black circles denote the position of the fluorescent probe in the mansyl-labeled DNA analogues.

The location of the polymerase catalytic site is much more ambiguous. The study of mutants with altered DNA polymerization capabilities (Joyce et al., 1985, 1986) and chemical modification studies (Mohan et al., 1988; Pandey & Modak, 1988) have shown that DNA interacts within the cleft in the large domain of the protein. Photoaffinity labeling experiments have identified Tyr766 (Joyce et al., 1986) and His881 (Pandey et al., 1987) as residues associated with the dNTP binding site and therefore necessarily proximate to the polymerase catalytic site.

Cocrystal X-ray structures of a duplex DNA–Klenow fragment complex have been difficult to obtain (Joyce & Steitz, 1987). On the basis of all the data available to date (mutant investigations, chemical modification studies, DNA footprinting, etc.), a DNA duplex has been model-built into the X-ray structure of the protein (Ollis et al., 1985). This structure places the polymerase catalytic site approximately 25 Å removed from the exonuclease catalytic site. A model has been proposed (Freemont et al., 1988; Figure 1) that allows these two spatially separated, functionally related catalytic activities to bind the DNA primer terminus, a property required for the editing function of the enzyme. In this model, sliding of the DNA duplex and melting of the four terminal base pairs occur, thus yielding a partially single-stranded primer bound at the exonuclease catalytic site of the enzyme. Duplex DNA remains bound within the large cleft of the protein. Experiments utilizing intrastrand cross-linked DNA have shown that approximately four bases of the duplex must be unpaired for hydrolysis of the primer terminus by the enzyme (Cowart et al., 1989).

An azidoDNA photoprobe has been synthesized in this laboratory (Gibson & Benkovic, 1987). Preliminary experiments have shown that this probe is an efficient substrate for the enzyme and that it can be used to label the protein in the presence of UV light. We now present a more detailed examination of the photolabeling of the Klenow fragment with this DNA photoprobe and identify Tyr766 as the amino acid residue modified when the probe resides at the polymerase catalytic site of the enzyme.

A fluorescent DNA probe useful in determining protein–DNA contacts has similarly been described (Allen et al., 1989). We now report the use of this modified duplex to probe the proposed editing mechanism of the enzyme. The data presented suggest that the primer terminus of the DNA duplex resides predominantly at the polymerase catalytic site and that the rate-limiting step in DNA degradation by the enzyme is the translocation of the primer terminus to the exonuclease catalytic site. The implications for the fidelity of DNA replication by the enzyme are discussed.

Experimental Procedures

Materials. Unlabeled nucleotides were purchased from Pharmacia. ^{32}P-Radiolabeled nucleotides were purchased from New England Nuclear. Mansyl chloride was purchased from

Chart I: Azido-Labeled DNA Analogues Utilized in These Studies[a]

11az/20mer	3′ AGCGTCGGCAGGTTCCCAAA 5′ 5′ TCGCAGCCGUC 3′	
10az/20mer	5′ TCGCAGCCGU	3′
12az/20mer	5′ TCGCAGCCGUCC	3′
14az/20mer	5′ TCGCAGCCGUCCAA	3′
17az/20mer	5′ TCGCAGCCGUCCAAGGG	3′
20az/20mer	5′ TCGCAGCCGUCCAAGGGTTT	3′
13/20mer	3′ AGCGTCGGCAGGTTCCCAAA 5′ 5′ TCGCAGCCGTCCA 3′	

U = 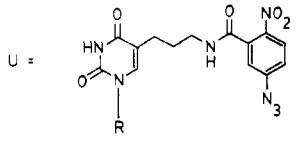

[a] For clarity, the 20mer template strand is shown explicitly only for the 11az/20mer.

Molecular Probes. 5′-Dimethoxytrityl 3′-β-cyanoethyl phosphoramidites were purchased from American Bionetics. Polynucleotide kinase was purchased from United States Biochemical Corp. Klenow fragment was purified as previously described (Joyce & Grindley, 1983) from *E. coli* strains kindly provided by Dr. C. Joyce. Protein concentration was determined spectrally, using $\epsilon_{278} = 6.32 \times 10^4$ M^{-1} cm^{-1} (Setlow et al., 1972). All other materials were of the highest quality commercially available.

Oligonucleotides. DNA oligomers were synthesized with an Applied Biosystems 380A DNA synthesizer. The oligonucleotides were deprotected, detritylated, and purified by gel electrophoresis. The synthesis and purification of fluorescent and photoreactive oligonucleotides have been previously reported (Allen et al., 1989; Gibson & Benkovic, 1987). Duplex formation was accomplished by mixing the primer strand with a slight excess (2–3%) of template strand at room temperature in the standard reaction buffer. The concentration of the individual strands was determined spectrally using extinction coefficients derived by summation of the extinction coefficients for each of the individual bases contained in the oligomers. 5′-^{32}P labeling of the DNA oligomers was accomplished as previously described (Mizrahi et al., 1986). The DNA substrates utilized in this study are shown in Charts I and II.

Electrophoresis and Sequencing Gel Analysis of Oligonucleotide Products. Preparative electrophoretic purification of the oligonucleotides was accomplished by fractionation on a denaturing (8 M urea) 20% polyacrylamide gel (3 mm × 18 cm × 36 cm). The DNA was visualized by UV shadowing and the major band excised from the gel with a razor blade. The gel material was crushed into a fine powder and extracted 3 times with 1 M TEAB (pH 7.0). The combined extracts were diluted 1:5 with water, desalted (Sep-Pak), and taken to dryness, and the residue was taken into 50 mM Tris-HCl (pH 7.5).

Chart II: Mansyl-Labeled DNA Analogues Utilized in These Studies[a]

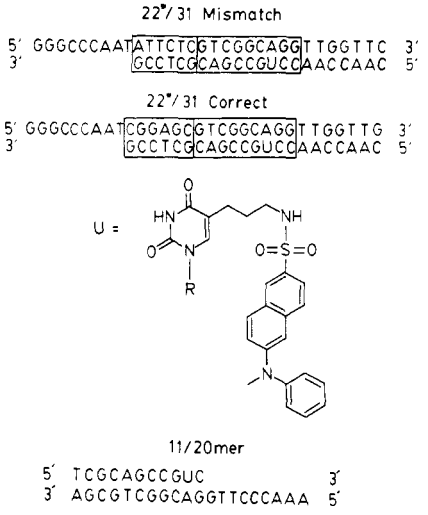

[a] The boxes delineate mismatched bases in the 22*/31mer-mismatch substrate (and the analogous matched bases in the correct oligonucleotide) as well as the extent of the duplex covered by the duplex binding site of the enzyme.

Analytical analysis of oligonucleotide products was accomplished by fractionation of the 5′-^{32}P-labeled oligonucleotides by electrophoresis on a denaturing (8 M urea) 15% polyacrylamide sequencing gel (0.4 mm × 32 cm × 40 cm), and the bands were visualized by autoradiography (Mizrahi et al., 1986). Proteins were analyzed on a denaturing (SDS) 12.5% polyacrylamide gel by the method of Laemmli (1970). Covalent radiolabeled DNA–protein complexes were similarly detected by autoradiography. Quantitation of all radioactive species was accomplished by excision of the appropriate bands and scintillation counting in 3 mL of Scintiverse II cocktail (Fisher). Alternatively, the autoradiograms were analyzed by densitometry utilizing a LKB scanning densitometer.

FPLC and HPLC. Both FPLC and HPLC chromatographic separations were performed on a Waters 990$^+$ chromatography workstation interfaced to a NEC powermate II computer for data capture. FPLC separations utilized a Pharmacia Mono-Q (5 × 50 mm) column equilibrated with 50 mM Tris-HCl (pH 7.5) buffer. Elution was accomplished with a KCl gradient to 600 mM over 60 min, followed by a 10-min gradient to 1 M KCl. Two reverse-phase HPLC separation protocols were used: (1) Peptide elution protocol utilized a Waters Delta Pak C-18 column (0.39 × 30 cm) equilibrated with 20 mM ammonium phosphates (pH 6.8) (buffer A). Elution was accomplished with buffer B (70% acetonitrile, 30% buffer A) at 0% for 5 min, 0–50% over 90 min, and 50–100% over 10 min. (2) Oligonucleotide elution protocol utilized a Waters Delta Pak C-4 column (0.39 × 30 cm) equilibrated with 5% acetonitrile in 100 mM TEAA (pH 7.0). Elution was accomplished with an acetonitrile gradient to 25% over 40 min. The flow rate in all cases was 1 mL/min.

Rate of Hydrolysis of 11az/20mer DNA by the Klenow Fragment. Enzyme (5 μM) was added to a slight (5%) excess of 5′-^{32}P-labeled 11az/20mer DNA in 50 mM Tris-HCl (pH 7.5) buffer containing 1 mM EDTA. The reaction was initiated with $MgCl_2$ to a final concentration of 10 mM and allowed to proceed in the dark at room temperature. Aliquots were removed at the indicated times, the reaction was quenched with the addition of an equal volume of sequencing gel load buffer, and the radioactive oligonucleotide products were analyzed by gel electrophoresis. The DNA products were excised from the gel and counted in Scintiverse II (Fisher). The rate of hydrolysis of the 11az/20mer was determined directly from these data. The rate of hydrolysis of the 10az/20mer was determined by kinetic simulation of the data.

Polymerization of 11az/20mer DNA by the Klenow Fragment and Photolabeling of the Protein. Enzyme (5 μM) was added to a slight (5%) excess of 5′-^{32}P-labeled 11az/20mer DNA in 50 mM Tris-HCl (pH 7.5) buffer containing 1 mM EDTA. Nucleotide triphosphates were included to 50 μM in nonidling base and 250 μM in idling base. Reactions were initiated with the addition of $MgCl_2$ to a final concentration of 10 mM and incubated for 90 s at room temperature. The samples were then photolyzed (Spectroline Model XX-15B UV lamp, 302-nm output maximum, no filters) at a distance of 5 cm for 2 min (16.2 mW/cm^2). The reaction was quenched with the addition of either an equal volume of sequencing gel load buffer or EDTA to a final concentration of 15 mM. DNA products were fractionated by sequencing gel and detected by autoradiography as described above. Photolabeled protein products were similarly analyzed by SDS–PAGE.

Preparative Photolabeling of the Klenow Fragment with 10az/20mer DNA. Enzyme (5 μM) and 11az/20mer DNA (5% excess, ten 1-mL aliquots) were incubated at room temperature for 30 min and then photolyzed for 2 min as described above. The reactions were then quenched with EDTA and the samples combined and concentrated to a volume of approximately 4.5 mL in vacuo (Savant Speed Vac). The mixture was then fractionated by FPLC (three 1.5-mL injections) and the eluent monitored with a diode array spectrophotometer. Analysis of the UV spectra of eluting species allowed the identification and isolation of unmodified protein, photolyzed DNA, and DNA-labeled protein. The photolyzed DNA thus isolated was 5′-^{32}P-labeled and analyzed by sequencing gel analysis. This confirmed that all of the DNA substrate was degraded to the 10az/20mer during the preincubation period.

Tryptic Digestion of the DNA-Labeled Klenow Fragment and Identification of the Labeled Amino Acid Residue. The DNA-labeled Klenow fragment isolated by FPLC (vide supra) was pooled, desalted (Centricon 30 microconcentrator), and buffer-exchanged into 1 mL of 50 mM Tris-HCl (pH 7.5). The amount of photolabeled protein was estimated by integration of the 220-nm chromatogram (see Figure 4). TPCK-treated trypsin was added and the mixture kept at 37 °C for 6 h. An additional aliquot of trypsin was added at 3 h (final trypsin:Klenow ratio was 1:20). The resultant peptides were fractionated at the end of the digestion period by utilizing the peptide elution protocol described above. Fractions (1 mL) were collected and DNA-labeled peptides rechromatographed by utilizing the oligonucleotide elution protocol also described above. DNA-labeled peptides were collected manually and submitted for N-terminal amino acid sequence analysis. Sequence analysis was performed with an Applied Biosystems 447A gas–liquid amino acid sequenator.

Fluorescent Measurements. All fluorescence measurements were performed on an SLM 8000C (SLM/Aminco, Urbana, IL). The excitation wavelength for all mansyl-labeled DNA samples was 340 nm. All samples contained 50 mM Tris-HCl (pH 7.4), 400 nM fluorescent duplex DNA, and 400 nM Klenow fragment in a final volume of 1 mL. $MgCl_2$ (5 mM) or EDTA (20 mM) was added to promote or inhibit, respectively, the exonuclease activity of the enzyme.

Binding of Fluorescent DNA to EpoxyATP-Inactivated Klenow Fragment. EpoxyATP (5 μM), 13/20mer duplex DNA (400 mM), and the Klenow fragment (400 nM) were

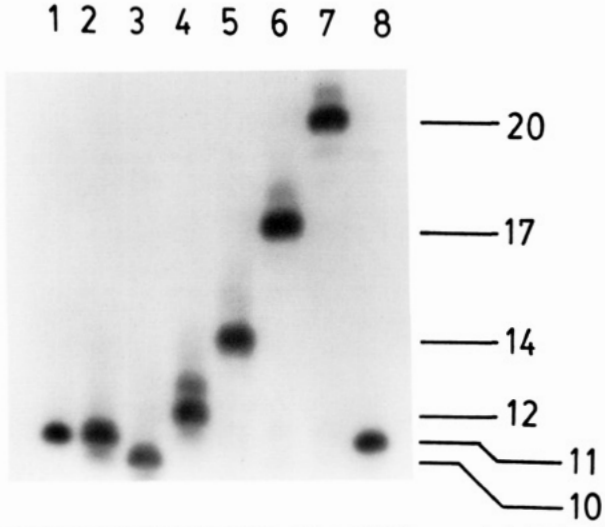

FIGURE 2: Effectiveness of 11az/20mer DNA as a substrate for the Klenow fragment. Autoradiogram of a DNA sequencing gel demonstrating effective exonuclease and polymerase activities on the azidoDNA substrate. Lanes 1 and 8, 11az/20mer DNA standard. Lanes 2 and 3, 11az/20mer DNA incubated with the Klenow fragment in the presence of EDTA and magnesium, respectively. Lane 4, same as lane 3 except dCTP was added to the incubation mixture. Lane 5, same as lane 3 except both dCTP and dATP were included. Lane 6, same as lane 3 except dCTP, dATP, and dGTP were included. Lane 7, same as lane 3 except all four dNTP's were added. Details of the incubations are given under Experimental Procedures.

added to 50 mM Tris-HCl (pH 7.4) containing 2 mM $MgCl_2$. After 15 min at 37 °C, 11*mer single-stranded DNA was added to a final concentration of 400 nM and the fluorescence emission spectrum recorded.

Kinetic Simulation and Computer Graphics. The GraphPAD program (ISI Software, Philadelphia, PA) was utilized for both linear and exponential curve fits. Kinetic simulations were performed by using a modified version of the program Simul (Barshop et al., 1983; Anderson et al., 1988). Computer graphics simulations were performed by using an Evans and Sutherland PS390 graphics workstation. Single-stranded oligonucleotides were built by using Tripos Associates Sybyl/Mendel programs. DNA duplexes were model-built manually and then minimized by using the Sybyl/Mendel programs. Protein–DNA structures were model-built manually.

RESULTS

Hydrolysis of the 11az/20mer by the Klenow Fragment. Due to the nature of automated DNA synthesis, oligonucleotide elongation occurs in the 3′ → 5′ direction. The 3′-terminal nucleotide is covalently attached to a solid support by its 3′-hydroxyl group and phosphoramidite nucleotides are sequentially added to the 5′-hydroxyl moiety of the growing chain. Given that the precursor to the azido-modified base is incorporated into the oligonucleotide as a phosphoramidite [see Gibson and Benkovic (1987)], placement of the azido probe directly at the primer terminus could not be achieved synthetically.

Incubation of the Klenow fragment with 11az/20mer DNA in the presence of magnesium results in the degradation of the primer strand (Figure 2). The 11az/20mer primer is hydrolyzed to the corresponding 10az/20mer at a rate (1.9×10^{-3} s^{-1}) similar to that observed with several other synthetic duplexes utilized in this laboratory (Kuchta et al., 1988). Subsequent hydrolysis of the azido-modified base, however, is slowed significantly (8×10^{-5} s^{-1}) and thus allows complete enzymatic conversion of the 11az/20mer to the 10az/20mer in situ.

Table I: Inhibition of Photolabeling by Competing 13/20mer DNA

13/20mer DNA (μM)	rel % labeling[a]
0	100
5	28
10	ND[b]

[a] 100% relative photolabeling represents approximately 40% of the protein modified with the DNA photoprobe. [b] ND, not detectable.

Table II: Photolabeling of the Klenow Fragment with AzidoDNA

base added	primer length	rel % labeling[a]
none	10mer	100
dCTP	12mer	31
dCTP, dATP	14mer	45
dCTP, dATP, dGTP	17mer	11
all four bases	20mer	9
−hν	11mer[b]	3

[a] 100% relative photolabeling represents approximately 40% of the protein modified with the DNA photoprobe. [b] The reaction mixture was kept in the dark and was not initiated with $MgCl_2$.

Photolabeling of the Klenow Fragment with 10az/20mer DNA. Photolysis of ^{32}P-radiolabeled 10az/20mer in the presence of the Klenow fragment results in radioactivity comigrating with the protein on an SDS–PAGE gel (data not shown). Photolysis times as short as 30 s result in significant labeling of the protein. Analysis of the radiolabeled DNA–protein complex by SDS–PAGE reveals that approximately 40% of the protein has been modified. Cooling of the photolysis mixture prior to and during photolysis has no effect on the extent of photolabeling. All experiments were therefore conducted at room temperature. Table I reveals that the addition of 13/20mer DNA to the photolysis mixture results in decreased photoyield, suggesting specificity for the DNA binding domain of the protein.

Figure 2 demonstrates that the 11az/20mer is an efficient substrate for the polymerase activity of the Klenow fragment. Addition of dNTP's to the photolysis mixture results in the elongation of the azido primer to the expected products (see Chart I). Table II reveals that both 12az/20mer and 14az/20mer DNA efficiently label the enzyme in the presence of UV light. Neither the 17az/20mer nor the 20az/20mer, however, yields significant photolabeling of the protein. The efficient elongation of the 17az/20mer to the 20az/20mer by the enzyme (Figure 2) suggests that binding of the DNA photoprobe to the enzyme is not significantly impaired and that the lack of labeling is due to translocation of the azido probe out of the DNA binding domain of the protein.

FPLC analysis of a mixture of prephotolyzed azidoDNA and the Klenow fragment yields the chromatogram shown in Figure 3A (upper trace). The electronic spectrum of the enzyme (Figure 3B) reveals maxima at 220 and 280 nm with a large 220 nm:280 nm ratio. The spectrum of the azidoDNA exhibits maxima at 210 and 260 nm with the 210 nm:260 nm ratio near unity. Additionally, the photolyzed DNA exhibits a weak absorbance maximum at 390 nm due to the photoprobe itself.

Photolysis of 10az/20mer DNA in the presence of the Klenow fragment results in two new species (A and B; Figure 3A, lower trace) not observed in enzyme or DNA. Concomitant with the appearance of these species is the loss of both enzyme and DNA. The electronic spectra of species A and B are identical (Figure 3B) and are consistent with a DNA-labeled protein: (1) a relatively large 210 nm:280 nm ratio, (2) a broad absorbance maxima extending over 260–280 nm,

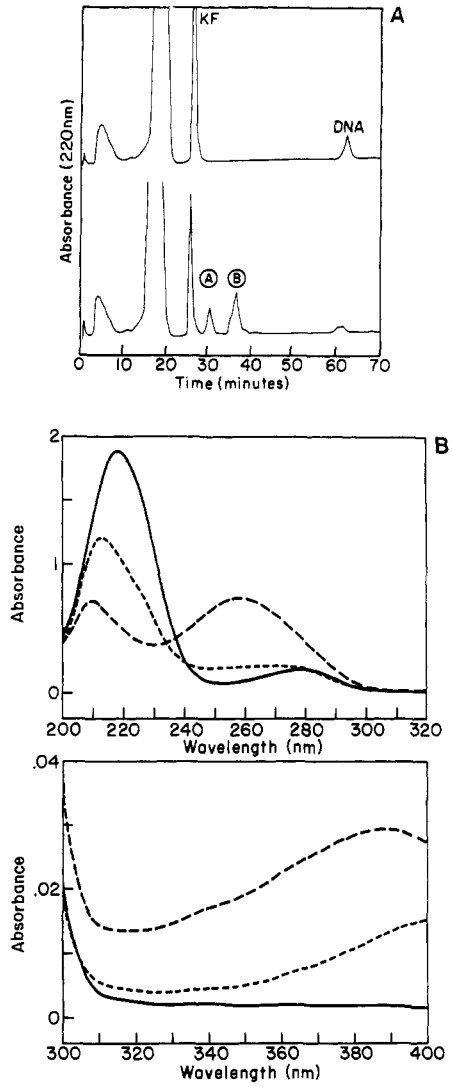

FIGURE 3: FPLC analysis of the Klenow fragment photolabeled with 10az/20mer DNA. (A) FPLC chromatogram of prephotolyzed azidoDNA mixed with enzyme (upper trace) and azidoDNA photolyzed in the presence of the Klenow fragment (lower trace). (B) Electronic spectra of enzyme (solid trace), photolyzed 10az/20mer DNA (long-dashed line), and photolabeled protein species A (panel A, lower trace). The electronic spectrum of photolabeled protein species B was identical with that of species A and is not shown here.

and (3) a weak absorbance maximum at 410 nm.

Preparative Photolabeling of the Klenow Fragment with the 10az/20mer and Identification of the Modified Amino Acid. Tryptic digestion of DNA-labeled protein (species A) followed by fractionation of the resulting peptides by HPLC yields the chromatograpm shown in Figure 4A. Identical results are obtained with species B and are not discussed separately. Although there are many closely eluting peptides (220-nm chromatogram), DNA-containing species are readily detected by a 260 nm:280 nm ratio >1 (DNA) and absorbance at 390 nm (photolyzed azido probe). Close inspection of the chromatogram in Figure 4 reveals three peaks with the necessary requirements. The first (arrow) has a retention time (41 min) and electronic spectrum (Figure 4B) identical with that of the photolyzed 10az/20mer DNA standard (not shown). This suggests that at least some of the labeled protein is unstable to the proteolysis procedure. The second two (1 and 2) elute with significantly longer retention times (65 and 70 min, respectively). Of note is that the electronic spectra of these two species (Figure 4B) exhibit absorbance maxima at 410 nm rather than the 390-nm maximum observed with

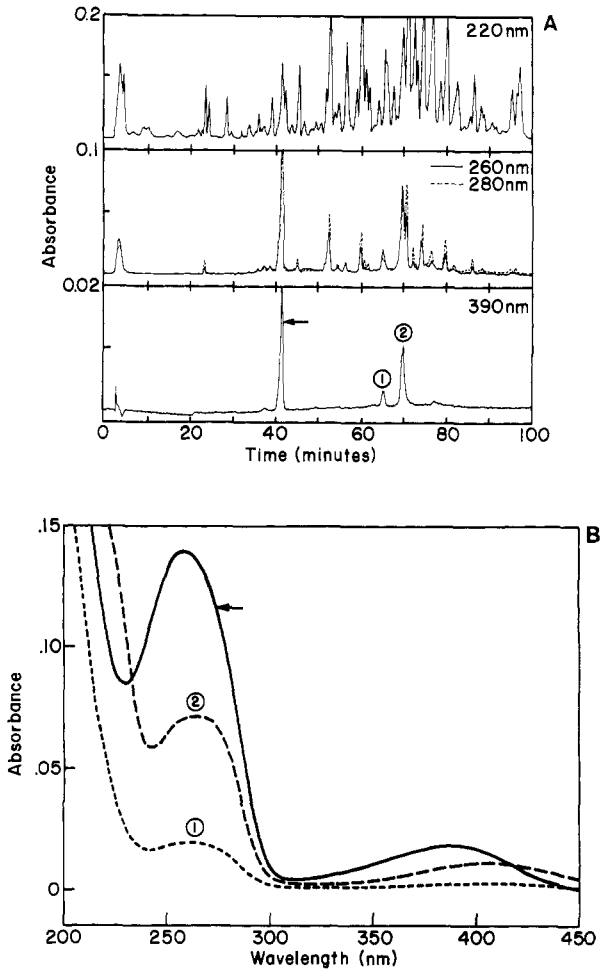

FIGURE 4: HPLC fractionation of peptides derived from trypsin digestion of the photolabeled Klenow fragment. Photolabeled protein species A (Figure 3) was digested with trypsin and fractionated as described under Experimental Procedures. (A) Three chromatograms are displayed: upper trace, all peptide fragments (220 nm); middle trace, DNA (260 nm) and aromatic amino acid containing peptides (280 nm); lower trace, photolyzed aryl azide probe (390 nm). (B) Electronic spectra of free DNA (solid line), peptide 1 (short-dashed line), and peptide 2 (long-dashed line). Identical results were obtained for photolabeled protein species B (Figure 3) and are not shown.

Table III: Amino Acid Sequence Analysis of Peptides I and II

cycle	amino acid	peptide I (pmol)	peptide II (pmol)
1	Ala	26	74
2	Ile	17	52
3	Asn	11.5	35
4	Phe	21.7	54
5	Gly	20.5	49
6	Leu	14.5	54
7	Ile	14.7	25
8	(Tyr)		
9	Gly	5.8	6
10	Met		2
11	Ser		9
12	end sequence data		

the photolyzed azidoDNA standard.

Further purification of peak 1 and peak 2 using the DNA purification protocol outlined under Experimental Procedures yields, in each case, a single DNA-containing species (data not shown). The electronic spectra of these peaks (not shown) are identical with those shown in Figure 4B. Both peak 1 and peak 2 were submitted for N-terminal amino acid sequence analysis, and the results are shown in Table III. The sequence unambiguously identifies the tryptic peptide fragment as

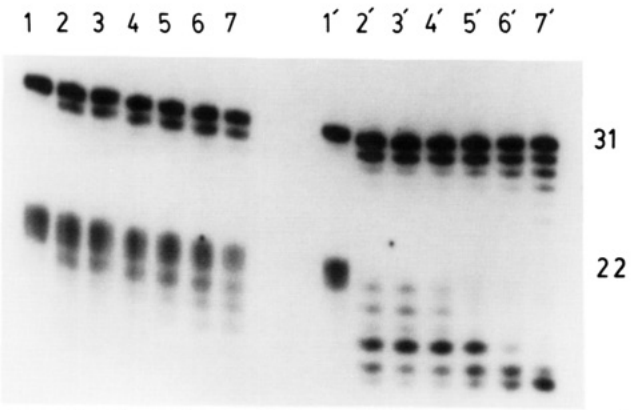

FIGURE 5: Exonuclease activity on 22*/31mer-correct (A) and 22*/31mer-mismatch (B) DNA by the Klenow fragment. Autoradiogram of the DNA fragments obtained by degradation of the DNA by the enzyme. Both the template strand and primer strand were 5′-^{32}P end labeled. Lanes 1 and 1′ are starting material standards. Lanes 2 through 7 and 2′ through 7′ represent 0.5-, 1-, 2-, 4-, 8-, and 16-min digest times, respectively. Details are given under Experimental Procedures.

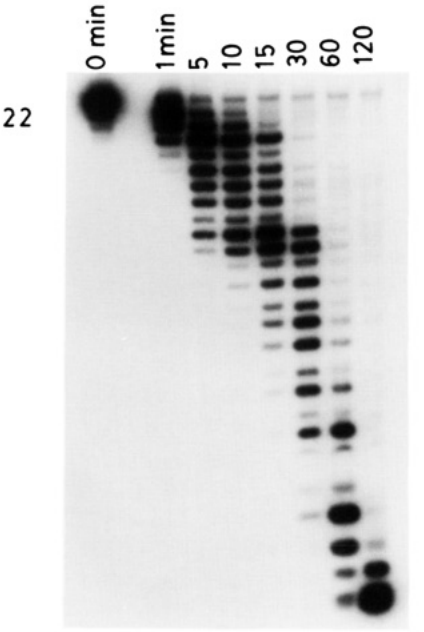

FIGURE 6: Exonuclease activity on 22*mer single-stranded DNA by the Klenow fragment. Autoradiogram of the DNA fragments obtained by degradation of the DNA by the enzyme. Lane 1 (0 min) represents the starting material standard. Details are given under Experimental Procedures.

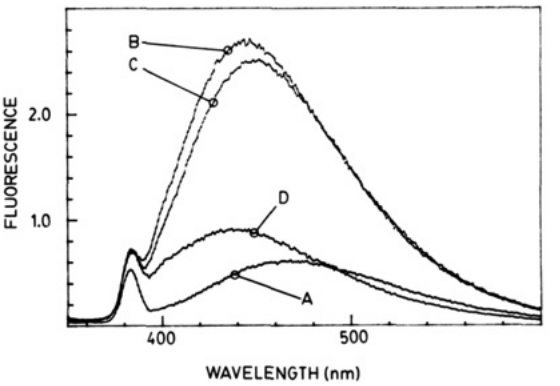

FIGURE 7: Fluorescence emission spectra of the 22*mer single-stranded DNA interaction with the Klenow fragment. (A) Spectrum of 22*mer single-stranded DNA alone. (B) Spectrum of DNA in the presence of the Klenow fragment and EDTA. (C) Spectrum of DNA in the presence of the Klenow fragment 2 min after the addition of magnesium. (D) Spectrum of DNA after 3 h of incubation in the presence of the Klenow fragment and magnesium. The DNA is completely degraded to monophosphates after 2 h (see Figure 6), and spectrum D resembles that of the mansyl-labeled nucleotide (not shown). Details are given under Experimental Procedures.

spanning (minimally) amino acid residues Ala759 to Arg775. The absence of any PTH-amino acid eluting in cycle 8 identifies the modified (DNA-labeled) residue as Tyr766.

Attempts to isolate DNA-labeled peptides resulting from photolysis of 12az/20mer and 14az/20mer DNA in the presence of the Klenow fragment were unsuccessful due to very low photoyield and instability of the labeled peptide, respectively.

Rationale for the Design of the Fluorescent DNA Probes. Approximately six to eight base pairs of duplex DNA are covered by the binding of the Klenow fragment to a DNA template-primer (Joyce et al., 1986). The placement of the mansyl-labeled base in the 22*/31-correct oligonucleotide duplex was chosen such that the binding of the primer terminus to the polymerase site would leave the fluorophore outside of the enzyme. Translocation of the primer terminus to the exonuclease site via the slide and melt model (Figure 1) requires approximately eight base pairs of duplex DNA to be drawn into the enzyme, thus placing the fluorophore in contact with the protein. Interaction of the mansyl probe with the enzyme results in an increased quantum yield of the fluorophore and enhanced fluorescence. The 22*/31-mismatch oligonucleotide duplex contains five terminal mismatched bases in an attempt to promote binding to the exonuclease site and placement of the fluorophore within the DNA binding site of the enzyme.

Hydrolysis of Mansyl-Labeled DNA by the Klenow Fragment. The fluorescent oligonucleotides utilized in this study are shown in Chart II. Incubation of mansyl-labeled DNA duplexes with the Klenow fragment in the presence of magnesium results in the degradation of the primer strand (Figure 5). While the degradation of fully duplexed mansyl-labeled polynucleotide (22*/31 correct) occurs only slowly, hydrolysis of mismatched (and presumably unpaired) bases occurs rapidly (22*/31 mismatch). Of note is that while four of the mismatched bases are removed in approximately 30 s, subsequent removal of the final mismatched base and correctly base-paired nucleotides occurs at a rate similar to that observed for the 22*/31-correct duplex. Exonucleolytic degradation of 22*mer single-stranded DNA by the enzyme (Figure 6) also occurs rapidly with a rate comparable to that observed for the hydrolysis of the mismatched bases in 22*/31-mismatch DNA.

Fluorescence Enhancement of Mansyl-DNA upon Binding to the Klenow Fragment. Addition of the Klenow fragment to 22*/31-mismatch DNA in the presence of EDTA (to inhibit the exonuclease activity of the enzyme) yields no increase in the fluorescence emission of the duplex (not shown). There was similarly no effect upon subsequent addition of $MgCl_2$.

Addition of 22*mer single-stranded DNA to the enzyme in the presence of EDTA results in significant enhancement of the fluorescence emission of the polynucleotide (Figure 7). Degradation of the DNA occurred upon addition of $MgCl_2$ (not shown) with a concomitant decrease in the fluorescence emission of the DNA probe (Figure 7).

The emission intensity of 11*mer single-stranded DNA is increased 6.6-fold with the addition of the Klenow fragment (Figure 8). Inactivation of the enzyme with epoxyATP and 13/20mer DNA results in duplex DNA tightly bound at the polymerase active site of the enzyme (Catalano & Benkovic, 1989). Addition of 11*mer to epoxyATP-inactivated Klenow

Chart III: Sequence Homology of the DNA Polymerases[a]

E. coli	Q R R S A K A I N F G L I **Y** G M S A F G L A R	-775
S. pneu	D R R N A K A V N F G V V **Y** G I S D F G L S N	-725
T. aquat	M R R A A K T I N F G V L **Y** G M S A H R L S Q	-680
Phage T5	L R Q A A K A I T F G I L **Y** G S G P A K V A H	-583
Phage T7	T R D N A K T F I Y G F L **Y** G A G D E K I G Q	-539

[a] Sequences are aligned to display homology about Tyr766 (bold) in all protein sequences.

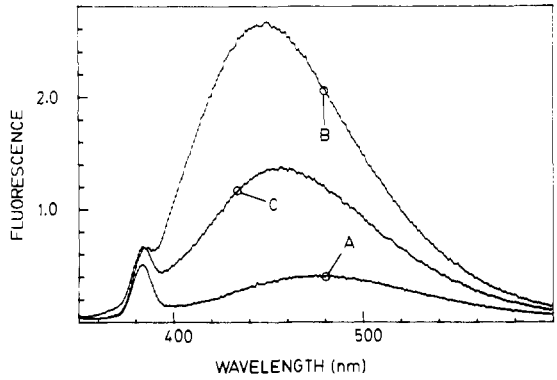

FIGURE 8: Fluorescence emission spectra of the 11*mer single-stranded DNA interaction with the epoxyATP-inactivated Klenow fragment. (A) Spectrum of 11*mer DNA alone. (B) Spectrum of 11*mer DNA in the presence of the Klenow fragment. (C) Spectrum of 11*mer DNA in the presence of epoxyATP-inactivated enzyme. Details are given under Experimental Procedures.

fragment similarly results in significant (3.4-fold) enhancement of fluorescence emission.

Discussion

The data presented in this paper clearly demonstrate that the 11az/20mer is an efficient substrate for the Klenow fragment of *E. coli* DNA polymerase I. Incubation of the azidoDNA photoprobe with enzyme results in degradation of the primer strnad by the 3′ → 5′ exonuclease activity of the enzyme (Figure 2). Interestingly, while the hydrolysis of the terminal base (dCMP; see Chart I) occurs at a rate (1.9×10^{-3} s^{-1}) similar to that observed for the degradation of a variety of synthetic template-primers utilized in this laboratory (Kuchta et al., 1988), the exonucleolytic hydrolysis of the azido-bearing base is significantly impaired (8×10^{-5} s^{-1}). This allows the formation of 10az/20mer DNA in situ, thus placing the azido photoprobe directly at the polymerase catalytic site. That the 11az/20mer is a substrate for the polymerase activity of the enzyme is also demonstrated in Figure 2. The primer strand of this azidoDNA duplex is efficiently elongated to the expected product in the presence of the appropriate combinations of dNTP's.

It has previously been shown that 11az/20mer DNA forms a covalent protein–DNA adduct in the presence of the Klenow fragment and UV light (Gibson & Benkovic, 1987). Table II reveals that 10az/20mer DNA also forms a covalent adduct when illuminated with UV light. The decrease in photoyield when 13/20mer DNA is added to the photolysis mixture (Table I) strongly suggests that this covalent cross-link occurs in the DNA binding pocket of the enzyme. That the labeling of the enzyme is highly specific for the duplex binding site is further evidenced by the formation of a covalent adduct with the 10az/20mer, the 12az/20mer, and the 14az/20mer but not the 17az/20mer or 20az/20mer DNA (Table II). Elongation of the primer strand by the enzyme results in the translocation of the azido-bearing base further into the duplex region of the DNA photoprobe. This in turn results in the translocation of the azido probe through and eventually out of the duplex DNA binding region of the protein. The data presented in Table II demonstrate that the DNA binding region of the enzyme covers at least five base pairs of duplex DNA since 14az/20mer DNA effectively labels the protein. The eighth base, however, must lie outside of the protein structure since no significant photolabeling of the enzyme occurs with 17az/20mer DNA. This argues that the duplex binding site extends between five and seven bases downstream from the polymerase catalytic site of the enzyme. This is in excellent agreement with DNA translocation experiments in which a fluorescent DNA probe was utilized to determine the extent of duplex bound by the enzyme (Allen et al., 1989) as well as DNase footprinting studies which determined six to eight bases of duplex DNA are protected by the protein (Joyce et al., 1986).

Illumination of 10az/20mer DNA with UV light in the presence of the Klenow fragment yields two photolabeled protein species (A and B, Figure 3A) readily separated by anion-exchange FPLC. Sequencing gel analysis of DNA isolated by FPLC reveals that the template strand is partially degraded during the preincubation period, yielding roughly equivalent amounts of 19mer and 20mer template (data not shown). Photolabeling of the enzyme with the resulting 10az/19mer–10az/20mer DNA mixture likely yields the observed FPLC species A and B, respectively.

Tryptic digestion of each of these photolabeled proteins yields an identical peptide map (Figure 4A), each with two DNA-labeled peptides. N-Terminal amino acid sequence analysis of each of these modified peptides yields, in all cases, a single sequence which unambiguously identifies the peptide as spanning (minimally) Ala759 to Arg775 in the Pol I amino acid sequence. The absence of a PTH-amino acid in cycle 8 of the sequence analysis identifies Tyr766 as the residue modified by the azidoDNA photoprobe. Given that the two peptides possess different retention times by RP-HPLC and yet yield identical N-terminal amino acid sequences, it is likely that one of the peptides represents an incomplete tryptic digestion of the peptide spanning Ala759 to Arg781 of the Pol I sequence.

Of note is that Tyr766 is also modified when the Klenow fragment is labeled with 8-azido-dATP, a photoreactive dNTP analogue (Joyce et al., 1986). This is not surprising given that the primer-terminus binding site and the dNTP binding site must be proximate for polymerization to occur. Furthermore, aryl azides are relatively selective in their reactions and have a propensity for aromatic amino acid residues (Baley & Staros, 1984).

Chart III shows the amino acid sequence of Pol I about Tyr766. Also shown are the sequences of *Streptococcus pneumoniae*, *Thermus aquaticus*, and phage T5 and T7 DNA

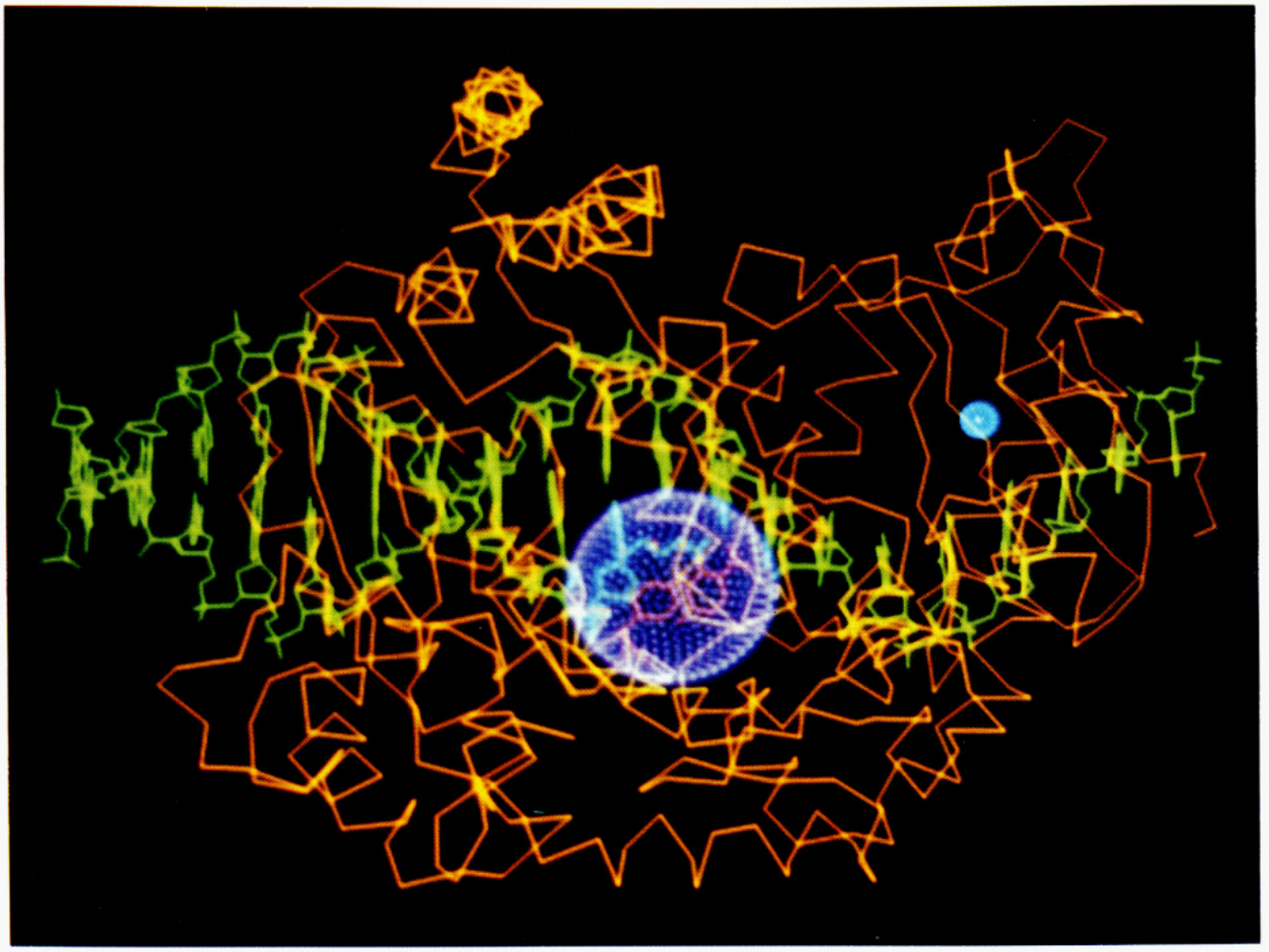

FIGURE 9: Proposed structure of the 10az/20mer photolabeled Klenow fragment. The structure was model-built as described under Experimental Procedures and is consistent with all the data currently available. The model shows Tyr766 and the azido photoprobe in red, the DNA in green, and the protein in amber. Approximately six bases of duplex DNA are covered by the protein structure. A 10-Å sphere centered at the modified tyrosine encompasses the polymerase site and accounts for the distance between the aromatic azide and the 3′-hydroxyl group at the primer terminus. Also shown is the location of metal site A (1-Å purple sphere) denoting the exonuclease catalytic site.

polymerases. The sequence homology between these four proteins is quite high overall (Lopez et al., 1989; Lawyer et al., 1989; Leavitt & Junetsu, 1989; Ollis et al., 1985), and the homology in this region is striking. Interestingly, Tyr766 and Gly767 are strictly conserved, as are several other of the residues in this region. Preliminary work on a Y766S mutant (kindly supplied by C. Joyce) indicates that this residue is fundamental in ensuring replication fidelity by the enzyme (S. Carroll, personal communication).

Figure 9 shows a computer graphics model-built complex of the 10az/20mer bound to the Klenow fragment. The location of the exonuclease catalytic site is indicated by a 1-Å sphere. The location of the polymerase catalytic site is similarly indicated by a 10-Å sphere centered about Tyr766 (shown in red). This figure clearly demonstrates the distance between the two catalytically linked sites.

The model presented for the editing mechanism of the enzyme (Figure 1) predicts that the DNA must slide toward the exonuclease site and melt approximately four base pairs of duplex DNA. Consequently, the duplex that lies just outside the DNA binding cleft is drawn into the protein structure. The amount of DNA movement while traversing the distance between the polymerase and exonuclease catalytic sites has been estimated at approximately seven to eight base pairs (Ollis et al., 1985; Cowart et al., 1989). Thus, a fluorescent probe appropriately placed in a DNA template-primer should exhibit background fluorescence when the 3′ end of the primer is bound at the polymerase site (mansyl probe outside of the protein) and fluorescence enhancement when bound at the exonuclease site (mansyl probe within the protein; see Figure 1).

Addition of mansyl-labeled single-stranded DNA to the Klenow fragment results in a significant increase in the emission intensity of the DNA (Figures 7 and 8), indicating that the mansyl probe now resides within the protein. No change in the emission spectrum was observed upon addition of either 22*/31-correct or 22*/31-mismatch DNA to the enzyme, indicating the fluorescent probe remains outside of the protein when the DNA is bound to the protein. These data clearly demonstrate that duplex DNA and single-stranded DNA interact with the protein quite differently. It is likely that single-stranded DNA does not interact significantly with the polar duplex binding domain of the enzyme but rather interacts with a separate, less polar site suited for interaction with the exposed hydrophobic bases. This is consistent with X-ray cocrystal structures of the Klenow fragment and duplex DNA. These structures show only single-stranded DNA bound at the exonuclease active site of the enzyme (Freemont et al., 1988). The high salt conditions utilized to form the crystals would tend to minimize polar interactions (and favor nonpolar interactions). That 11*mer single-stranded DNA interacts strongly with epoxyATP-inactivated enzyme (Figure

8) provides further support for this suggestion. Inactivation of the Klenow fragment with epoxyATP and 13/20mer DNA results in a binary complex with DNA bound tightly at the polymerase site of the enzyme (Catalano & Benkovic, 1989). Interaction of single-stranded DNA with the enzyme must therefore occur at a separate DNA binding site.

The rapid hydrolysis of four mismatched bases upon addition of $MgCl_2$ to the 22*/31-mismatch DNA–Klenow complex (Figure 5) suggests that the primer terminus can quickly shuttle to the exonuclease catalytic site of the enzyme. The inability to detect significant fluorescence enhancement with 22*/31-mismatch DNA is in accord with an equilibrium between the two sites highly favoring 3′-primer residence in the polymerase site. Exclusive or predominant binding at the exonuclease site would require sliding of the duplex, thus drawing the probe into the protein and enhancement of the probes' fluorescence emission (Figure 1, Chart II).

The exonuclease rate on the first four (mismatched) bases of 22*/31-mismatch DNA is extremely rapid with a rate similar to that observed for 22*mer single-stranded DNA (Figures 5 and 6). Subsequent hydrolysis occurs only slowly with a rate approximating that observed with fully duplexed 22*/31-correct DNA (Figure 5). These data suggest that the rate-limiting step in the exonuclease activity of the enzyme may involve DNA melting and translocation of the primer terminus between the two sites of the enzyme. Alternatively, 22*/31-mismatch DNA may bind aberrantly to the enzyme with the mismatched single-stranded 3′-primer terminus bound at the exonuclease site and the duplex region of the DNA in solution. We cannot yet distinguish between these two possibilities, but experiments are in now progress aimed at resolving this question.

Previous work in this laboratory (Kuchta et al., 1988) has demonstrated that the addition of nucleotides onto a correctly base-paired primer terminus is rapid (50 s^{-1}) while elongation of a mismatched primer terminus occurs only very slowly (10^{-5} s^{-1}). This may be central to the proofreading function of the enzyme. Polymerization onto a correctly base-paired primer terminus occurs rapidly without exonuclease intervention. The pause in polymerization onto a mismatched primer terminus may allow time for melting and translocation to the exonuclease site to occur. Once bound, hydrolysis of the terminal base occurs rapidly, thus excising the incorrectly incorporated base. Return of the primer terminus to the polymerase site occurs rapidly, and processive polymerization again proceeds without interruption.

This model explains how such a slow (10^{-3} s^{-1}; Kuchta et al., 1989) exonuclease activity may provide the proofreading function for a fast (50 s^{-1}; Kuchta et al., 1988) polymerase activity. The model also explains why a single mismatched base is removed at a rate similar to that of a correctly duplexed base (10^{-3} s^{-1}; Kuchta et al., 1989). In both cases, the rate of hydrolysis is limited by melting and sliding of the duplex. The observed exonuclease rate of 10^{-3} s^{-1} may therefore present melting and sliding between the two catalytic sites.

Acknowledgments

We gratefully acknowledge Dr. Katharine Gibson for her generous gift of the phosphoramidite nucleotide precursor utilized in the synthesis of both the azido- and mansyl-labeled DNA substrates. We thank Dr. Paul Reiss and Bob Bore of the DNA and Protein Chemistry Laboratory at The Pennsylvania State University Biotechnology Institute for their efforts in the peptide sequencing performed in this study. We are indebted to Dr. Randy Zauhar of the Biocomputing Center at the Biotechnology Institute for his help and patience in the generation of the computer graphics structures presented here.

Registry No. DNA polymerase, 9012-90-2; Tyr, 60-18-4.

References

Allen, D. J., Darke, P. L., & Benkovic, S. J. (1989) *Biochemistry 28*, 4601–4607.

Anderson, K. S., Sikorski, J. A., & Johnson, K. A. (1988) *Biochemistry 27*, 7395–7404.

Baley, H., & Staros, J. V. (1984) in *Azides and Nitrenes. Reactivity and Utility* (Scriven, E. F. V., Ed.) p 458, Academic Press, New York.

Barshop, B. A., Wrenn, R. F., & Frieden, C. (1983) *Ann. Biochem. 130*, 134–145.

Brutlag, D., Atkinson, M. R., Setlow, P., & Kornberg, A. (1969) *Biochem. Biophys. Res. Commun. 37*, 982–989.

Catalano, C. E., & Benkovic, S. J. (1989) *Biochemistry 28*, 4374–4382.

Cowart, M., Gibson, K. J., Allen, D. J., & Benkovic, S. J. (1975) *Biochemistry 28*, 1975–1983.

Derbyshire, V., Freemont, P. S., Sanderson, M. R., Beese, L., Freedman, J., Joyce, C. M., & Steitz, T. A. (1988) *Science 240*, 199–201.

Freemont, P. S., Friedman, J. M., Beese, L. S., Sanderson, M. R., & Steitz, T. A. (1988) *Proc. Natl. Acad. Sci. U.S.A. 85*, 8924–8928.

Gibson, K. J., & Benkovic, S. J. (1987) *Nucleic Acids Res. 15*, 6455–6467.

Jovin, T. M., Englund, P. T., & Bertsch, L. L. (1969) *J. Biol. Chem. 224*, 2996–3007.

Joyce, C. M., & Grindley, N. D. F. (1983) *Proc. Natl. Acad. Sci. U.S.A. 80*, 1830–1834.

Joyce, C. M., & Steitz, T. A. (1987) *Trends Biochem. Sci. 12*, 288–292.

Joyce, C. M., Fujii, D. M., Laks, H. S., Hughes, C. M., & Grindley, N. D. F. (1985) *J. Mol. Biol. 186*, 283–293.

Joyce, C. M., Ollis, D. L., Rush, J., Steitz, T. A., Konigsburg, W. H., & Grindley, N. D. F. (1986) *Protein Structure, Function and Design. UCLA Symposia on Molecular and Cellular Biology* (Oxender, D., Ed.) Vol. 32, pp 197–205, Alan R. Liss, New York.

Klenow, H., & Henningsen, I. (1970) *Proc. Natl. Acad. Sci. U.S.A. 65*, 168–175.

Kornberg, A. (1980) *DNA Replication*, W. H. Freeman, San Francisco, CA.

Kuchta, R. D., Mizrahi, V., Benkovic, P. A., Johnson, K. A., & Benkovic, S. J. (1987) *Biochemistry 26*, 8410–8417.

Kuchta, R. D., Benkovic, P. A., & Benkovic, S. J. (1988) *Biochemistry 27*, 6716–6725.

Laemmli, U. K. (1970) *Nature 227*, 680–685.

Lawyer, F. C., Stoffel, S., Randall, K. S., Myambo, K., Drummond, R., & Gelfond, D. H. (1989) *J. Biol. Chem. 264*, 6427–6437.

Leavitt, H. C., & Junetsu, I. (1989) *Proc. Natl. Acad. Sci. U.S.A. 86*, 4465–4469.

Lopez, P., Martinez, S., Diaz, A., Espinosa, M., & Lacks, S. A. (1989) *J. Biol. Chem. 264*, 4255–4263.

Mizrahi, V., Benkovic, P. A., & Benkovic, S. J. (1986) *Proc. Natl. Acad. Sci. U.S.A. 83*, 5769–5773.

Mohan, P. M., Basu, A., Basu, S., Abraham, K. I., & Modak, M. J. (1988) *Biochemistry 27*, 226–233.

Ollis, D. L., Brick, P., Hamlin, R., Xuong, N. G., & Steitz, T. A. (1985a) *Nature 313*, 762–766.

Ollis, D. L., Kline, C., & Steitz, T. A. (1985b) *Nature 313*, 818–819.

Pandey, V. N., & Modak, M. J. (1988) *J. Biol. Chem. 263*, 6068–6073.

Pandey, V. N., Williams, K. R., Stone, K. L., & Modak, M. J. (1987) *Biochemistry 26*, 7744–7748.
Que, B. G., Downey, K. M., & So, A. G. (1978) *Biochemistry 17*, 1603–1606.
Setlow, P., & Kornberg, A. (1972) *J. Biol. Chem. 247*, 232–240.
Warwicker, J., Ollis, D., Richards, F. M., & Steitz, T. A. (1985) *J. Mol. Biol. 186*, 645–649.

A Nucleotide That Enhances the Charging of RNA Minihelix Sequence Variants with Alanine†

Jian-Ping Shi, Christopher Francklyn, Kelvin Hill,‡ and Paul Schimmel*
Department of Biology, Massachusetts Institute of Technology, Cambridge, Massachusetts 02139
Received January 17, 1990; Revised Manuscript Received February 15, 1990

ABSTRACT: We showed earlier that a single G3·U70 base pair within the amino acid acceptor helix is a major determinant of the identity of $tRNA^{Ala}$. In addition, we demonstrated that an RNA hairpin minihelix that recreates the 12 base pair acceptor–TψC stem of $tRNA^{Ala}$ is also aminoacylated in a G3·U70-dependent manner. Determinants for efficient aminoacylation at pH 7.5 have been further investigated with minihelix substrates that have sequence variations at 3·70 and other locations. Although a U,U mismatch and other 3·70 nucleotide alternatives to G·U were recently proposed by others as also important for alanine acceptance, neither that mismatch nor any of four other 3·70 nucleotide combinations confer aminoacylation in vitro with alanine, even with substrate levels of enzyme. In contrast, permutations of the so-called discriminator nucleotide N73 (at position 73) strongly modulate, but do not block, aminoacylation of those substrates that encode G3·U70. In particular, the efficiency of G3·U70-dependent aminoacylation with alanine is strongly enhanced by having the wild-type A73. The effect of N73 alone can explain most of the difference in aminoacylation efficiency of a G3·U70-containing tRNA and a minihelix substrate whose sequences vary significantly from their $tRNA^{Ala}$ counterparts. Comparison with earlier work suggests that the substantial modulating effect of N73 is partly or completely obscured when N73 tRNA variants are expressed as amber suppressors in vivo.

For cells to preserve the fidelity of protein synthesis, tRNAs must be aminoacylated exclusively with their cognate amino acids. Recently, the sequence elements involved in establishing the identity of a tRNA have been investigated for several different tRNAs (Schimmel, 1989; Normanly & Abelson, 1989). From these studies, the acceptor stem and the anticodon have emerged as two regions where identity elements are concentrated (Hou & Schimmel, 1988; Schulman & Pelka, 1988, 1989; Sampson et al., 1989; Francklyn & Schimmel, 1989; Rould et al., 1989). In $tRNA^{Ala}$, the G3·U70 base pair in the amino acid acceptor helix acts as a major determinant of alanine identity (Hou & Schimmel, 1988; Francklyn & Schimmel, 1989; Park et al., 1989; Hou & Schimmel, 1989a,b). Because G3·U70 is unique to $tRNA^{Ala}$ (Sprinzl et al., 1989), it can in principle be used to distinguish that tRNA from all others. When introduced into $tRNA^{Cys}$, $tRNA^{Phe}$, and $tRNA^{Tyr}$ amber suppressors, the G3·U70 base pair confers on each of the host tRNAs the ability to insert alanine at a UAG codon (Hou & Schimmel, 1988, 1989b; McClain & Foss, 1988). In addition, RNA footprinting studies demonstrated that alanine tRNA synthetase protects nucleotides along the 3′ side of the acceptor stem and the unpaired CCA terminus of $tRNA^{Ala}$, but does not shield the anticodon at all (Park & Schimmel, 1988).

More recently, we demonstrated that small synthetic RNA helices whose sequences are based on a limited portion of the sequence of $tRNA^{Ala}$ are excellent substrates for alanine tRNA synthetase. A minihelix based on the acceptor–TψC stem of $tRNA^{Ala}$ is efficiently aminoacylated at a rate comparable to that of $tRNA^{Ala}$ (Francklyn & Schimmel, 1989). Substitution of G·C for the G3·U70 base pair abolishes aminoacylation with alanine. Also, transplantation of the G3·U70 base pair into a minihelix based on the acceptor–TψC sequence of $tRNA^{Tyr}$ confers alanine acceptance in vitro. Significantly, the G3·U70 $minihelix^{Tyr}$ has almost the same kinetic parameters for aminoacylation as a full-length $tRNA^{Tyr}$ into which the G3·U70 base pair has been transplanted (Francklyn & Schimmel, 1989; Hou & Schimmel, 1989b). This suggested that, in full-length $tRNA^{Tyr}$, the 49 nucleotides that are outside the acceptor–TψC stem do not perturb the interaction of the enzyme with the minihelix segment (acceptor–TψC stem) of the tRNA.

Because the minihelix substrates respond to substitutions at the 3·70 position in a manner indistinguishable from that of the full-length tRNA, we have used them to investigate further the basis of molecular recognition between $tRNA^{Ala}$ and its cognate synthetase. In particular, prior work has left unresolved two important questions concerning the role of the G3·U70 base pair in establishing alanine identity. First, McClain et al. (1988) observed weak in vivo suppression of an amber codon in a β-galactosidase mRNA by variants of $tRNA^{Ala}$ that encode alternative bases at the 3·70 position, including the U3·G70 transversion and the U3,U70 mismatch. This raised the possibility that a helical irregularity at the 3·70 position can, to a low extent, confer alanine acceptance. However, studies with the U3·G70 variant of $tRNA^{Ala}$, and with the A3·U70 and G3·C70 variants, failed to demonstrate any in vitro aminoacylation with alanine, even after prolonged incubation of each variant with substrate levels of enzyme

†Supported by Grant GM 15539 from the National Institutes of Health.
*To whom correspondence should be addressed.
‡Present address: Department of Biochemistry, School of Medicine, Loma Linda University, Loma Linda, CA 92350.

0006-2960/90/0429-3621$02.50/0